








Analyzing Cognitive Patterns in Gifted Children Using MRI and Morphometric Similarity Networks

Shuning Han^{1,2} ^a, Feng Duan³ ^b, Gemma Vilaseca^{4,5} ^c, Núria Vilaró⁵ ^d, Cesar F. Caiafa⁶ ^e,
Zhe Sun^{2,7} ^f and Jordi Solé-Casals^{1,8} ^g

¹Data and Signal Processing Research Group, University of Vic-Central University of Catalonia, Vic, Catalonia, Spain

²Image Processing Research Group, RIKEN Center for Advanced Photonics, RIKEN, Wako-Shi, Saitama, Japan

³Tianjin Key Laboratory of Brain Science and Intelligent Rehabilitation, Nankai University, Tianjin, China

⁴Psychological Department, Oms and Prat school, Fundació Catalunya - La Pedrera, Manresa, Catalonia, Spain

⁵Oms Foundation, Manresa, Catalonia, Spain

⁶Instituto Argentino de Radioastronomía-CCT La Plata, CONICET / CIC-PBA / UNLP, Argentina

⁷Faculty of Health Data Science, Juntendo University, Urayasu, Chiba, Japan

⁸Department of Psychiatry, University of Cambridge, Cambridge, U.K.


Keywords: Gifted Children, Structural Magnetic Resonance Imaging, Morphometric Similarity Network, Connection Density, Anatomical Modularity, Topological Features.


Abstract: Advances in non-invasive neuroimaging, such as structural magnetic resonance imaging (sMRI), have enabled the construction of structural brain networks (SBNs), allowing in vivo mapping of anatomical connections. This study investigates brain network structural differences linked to different intelligence levels in children by individual morphometric similarity networks (MSNs) derived from sMRI data. Through group- and individual-level analyses, we aim to uncover key topological features associated with cognitive performance and to identify a suitable connection density for SBN analysis. Connection density strongly affects global and nodal topological features, with a range of $p = 0.05$ to 0.15 recommended for stable and optimal results. Gifted individuals exhibit stronger intra-hemispheric and intra-modular connectivity, a more balanced distribution of left-to-right intra-hemispheric connections, and lower mean versatility, supporting efficient and stable cognitive processing. Moreover, anatomical modularity analyses based on von Economo indicate that higher cognitive performance is linked to enhanced connectivity in specific areas (such as secondary sensory area, motor to association area and secondary sensory to limbic area), alongside selective reduction in certain modular connections (such as motor to insular area, association to secondary sensory area and motor to secondary sensory area). Furthermore, topological features, including participation coefficient and local efficiency, are linked to cognitive performance. These findings provide valuable insights into the SBNs underlying cognitive levels in children.


1 INTRODUCTION


Understanding the neural basis of cognitive abilities has long been a key goal in cognitive neuroscience. Despite considerable progress, significant gaps remain, particularly in understanding the structural and functional differences in the brains of gifted individ-


uals. A promising approach to bridging this gap is the study of brain networks, which explores the connectivity and interactions among different brain regions. Recent advances in non-invasive neuroimaging techniques, such as structural magnetic resonance imaging (sMRI) and diffusion MRI, have enabled researchers to map these anatomical connections in vivo (Genon et al., 2022; Lo et al., 2011). These techniques allow for the construction of structural brain networks (SBNs), where the brain is modeled as a graph composed of nodes (brain regions) and edges (connections between them), providing a foundation for applying graph theory to explore the brain's organization and its relationship to cognitive abilities (Faskowitz et al.,


^a  <https://orcid.org/0009-0004-0792-5484>


^b  <https://orcid.org/0000-0002-2179-2460>

^c  <https://orcid.org/0000-0002-7533-2355>

^d  <https://orcid.org/0000-0002-7273-6039>

^e  <https://orcid.org/0000-0001-5437-6095>

^f  <https://orcid.org/0000-0002-6531-0769>

^g  <https://orcid.org/0000-0002-6534-1979>

2022).

Two main approaches are used to construct SBNs: tractography from diffusion-weighted imaging (DWI) and structural covariance networks (SCNs) derived from sMRI. SCNs traditionally compute the covariance of a single morphometric feature, such as cortical thickness, between regions across a group of subjects (Solé-Casals et al., 2019). While this method has been invaluable in understanding group-level brain organization, recent advances have introduced individual-level SCNs, allowing for a more detailed, personalized view of brain structure by incorporating multiple morphometric features (Kong et al., 2015; Li et al., 2017; Yu et al., 2018; Seidlitz et al., 2018; Li et al., 2021; Sebenius et al., 2023; Sun et al., 2024a,b). A notable development in this field is the morphometric similarity network (MSN) (Seidlitz et al., 2018), which constructs individual brain networks using multiple structural features derived from sMRI. MSNs are based on the pairwise correlations of morphometric feature vectors between brain regions, facilitating a more granular investigation of the brain’s structural organization. This method has shown promise in revealing biologically relevant patterns in brain networks.

Previous research has uncovered distinct patterns in SBNs associated with various biological characteristics, such as gender (Sun et al., 2015), cognitive ability (Park and Friston, 2013) and neurodegenerative diseases progression (Sun et al., 2024b). Despite these advances, key questions remain unanswered. How do the topological properties of MSNs relate to cognitive performance, particularly in children? How do modular and hemispheric specializations contribute to neural efficiency in gifted individuals? How do different connection densities affect brain network properties? These questions are critical for understanding the structural underpinnings of cognitive abilities.

This study addresses these gaps by constructing MSNs from sMRI data and analyzing their topological features in relation to cognitive performance in both gifted and control groups. Specifically, we conduct a comprehensive group comparison analysis, focusing on modular connections based on von Economo (VE) (Von Economo, 1929), the effects of different connection densities, intra-/inter-modular connections based on VE and intra-/inter-hemispheric connections. We also explore how nodal, global topological features and specific VE-Region connections are linked to cognitive performance. By combining group-level and individual-level analyses, this study offers new insights into the neural mechanisms of giftedness, emphasizing the role of anatomical mod-

ularity, hemispheric specialization, and topological features in efficient cognitive processing.

The rest of this paper is structured as follows: Section 2 outlines the dataset and methods employed. Section 3 presents the results of our analyses, which are discussed in Section 4. Finally, Section 5 concludes the study.

2 MATERIALS AND METHODS

2.1 Data

2.1.1 Participants

In this study, we use the dataset consisting of sMRI and cognitive tests from 29 healthy right-handed male participants with no history of psychiatric or neurological disorders (Solé-Casals et al., 2019). The raw (anonymized) MRI data and cortical thickness data are accessible in the OpenNeuro repository at <https://openneuro.org/datasets/ds001988>.

The participants are categorized into two groups: a control group (CG, 14 subjects) and a gifted group (GG, 15 subjects). Details of the participants’ information can be found in Table 1. The table indicates no significant age differences but significant difference in full-scale IQ between the groups.

Table 1: Participant information.

Groups	CG (Mean±SD)	GG (Mean±SD)
Age	12.53 ± 0.77	12.03 ± 0.54
IQ	122.71 ± 3.89	148.80 ± 2.93

2.1.2 sMRI Data

MRI scans were performed on a 3T scanner, yielding high-resolution T1-weighted images obtained via the MPRAGE 3D protocol. In this study, we adopted the sMRI preprocessing method outlined in prior research (Solé-Casals et al., 2019). FreeSurfer v5.3 was used for preprocessing to estimate cortical thickness from a three-dimensional cortical surface model based on intensity and continuity information (Fischl and Dale, 2000). Cortical reconstructions were independently reviewed by two experienced researchers to ensure adherence to quality control criteria. Each brain was parcellated into 308 ($R = 308$) regions (approximately 500 mm^2 each) using the standard FreeSurfer template (fsaverage) by a backtracking algorithm, which subdivides the regions defined in the Desikan-Killiany atlas (Desikan et al., 2006). The surface-based (non-linear) registration by the FreeSurfer com-

mand `mri_surf2surf` was then applied to warp the parcellation from the standard template to each individual's native MPRAGE space (Ghosh et al., 2010).

The 308 parcellated regions are classified into seven cytoarchitectonic cortical types based on the VE classification (Von Economo, 1929). Concisely, structural *type1* encompasses regions with minimal laminar differentiation, notably the primary motor cortex/precentral gyrus. Structural *type2* and *type3* generally include association cortices, while structural *type4* and *type5* correspond to secondary and primary sensory areas, respectively. The original VE classification of structural types does not differentiate between true six-layered isocortex and mesocortex or allocortex, which exhibit distinct cytoarchitectures and ontogenies. Consequently, we introduced two additional subtypes: *type6*, the limbic cortex, encompassing the entorhinal, presubicular, retrosplenial, and cingulate cortices and primarily constitutes allocortex; and *type7*, the insular cortex, including agranular, dysgranular and granular regions (Solé-Casals et al., 2019; Seidlitz et al., 2018; Váša et al., 2018; Vértes et al., 2016). In this study, we conduct anatomical modularity analyses based on VE-Regions.

2.2 Methods

In this study, we construct MSNs from sMRI data. Group-level analyses are performed by comparing the average MSNs of the CG and GG to identify key differences in brain network topology. Additionally, we conduct individual-level analyses to explore the relationship between cognitive performance and the structural organization of brain networks.

2.2.1 Network Construction

In this study, we construct brain networks for each subject using the morphometric similarity network (MSN), which represents the structural connectivity between brain regions (Seidlitz et al., 2018). The MSN converts each individual's set of multimodal MRI features into a morphometric similarity matrix of pairwise inter-regional correlations of morphometric feature vectors. In this study, as depicted in Fig. 1, a set of d ($d = 5$) morphometric features (308×5 for each sample) derived from any T1-weighted MRI scans: total surface area (tSA), total gray matter volume (tGMV), average cortical thickness (aCT), integrated rectified mean curvature (iMC), integrated rectified (Gaussian) curvature (iGC), was employed to construct MSNs. It has been demonstrated that the MSNs based on these five features are similar to MSNs utilizing a broader array of features (Seidlitz

et al., 2018), with tSA, tGMV, aCT, and iGC identified as the most discriminative features (Zhang et al., 2021). Following prior studies (Li et al., 2017; Seidlitz et al., 2018), each feature vector is standardized by the z-score values before the correlation calculation. Nodes in the MSN correspond to the 308 regions defined by the atlas. Edges are constructed based on the morphometric similarity between each possible pair of regions, quantified using the Pearson's correlation coefficient (PCC) between their normalized morphometric feature vectors. Each sample's MSN is represented as a weighted, undirected graph, where the 308×308 adjacency matrix contains PCC values as edge weights. A PCC value close to -1 denotes anti-correlation between the pair of features, while a PCC value close to 1 denotes strong correlation between the pair of features (Heinsfeld et al., 2018). Hence, the diagonal elements of MSN equal to 1. However, we uniformly assign NaN values to the diagonal elements of MSNs.

2.2.2 Group Comparison Analyses for MSNs

As shown in Fig. 1, we compute the average brain networks for the two groups, CG and GG. In this section, we present a comparative analysis of these group-level networks. The brain networks are first reorganized into 7 VE-Regions. To identify significant differences in connections between CG and GG average networks, we use the Mann-Whitney U test, a non-parametric statistical method suitable for small samples and non-normal distributions. Additionally, the analysis of the networks across different densities is conducted using the minimum spanning tree (MST) method to ensure full connectivity. Furthermore, we investigate the nodal topological features of the networks, quantifying the differences between the two groups through Euclidean distance. Moreover, we examine intra-/inter-VE connections and intra-/inter-hemispheric connections for CG and GG at a specific connection density.

- **VE-Region analysis for group brain networks.**

Firstly, the brain networks are reordered according to the 7 VE-Regions. The connections between VE-Region k and l in a brain network \mathcal{A} are defined as

$$\mathcal{A}^{kl} = \mathcal{A}_{ij} \quad (i \in N^k, j \in N^l, i \neq j) \quad (1)$$

where \mathcal{A}^{kl} represents the connections of brain network between nodes in VE-Region k and nodes in VE-Region l , with $k, l = 1, 2, \dots, 7$; N^k and N^l denote the sets of nodes in VE-Regions k and l , respectively. When $k = l$, \mathcal{A}^{kl} denotes intra-VE connections, while for $k \neq l$, it denotes inter-VE connections.

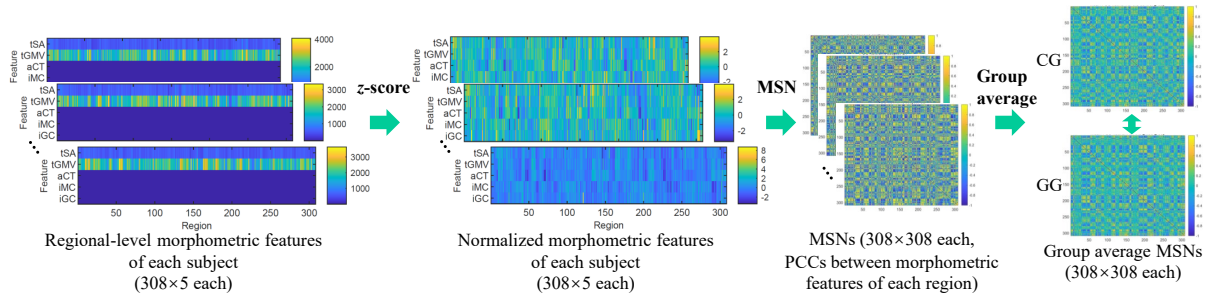


Figure 1: MSN construction and processing for group average MSNs. Five morphometric features (tSA, tGMV, aCT, iMC, iGC) are extracted from each brain region, resulting in 308×5 features per sample. These features are normalized using the z-score method. MSNs (308×308) are then computed by calculating the PCCs between the normalized features of all region pairs. Finally, group average MSNs are generated for both CG and GG.

The average VE connection or VE connection strength \mathcal{E} (7×7) of a brain network \mathcal{A} can be defined as

$$\mathcal{E}(k, l) = \frac{1}{n_{kl}} \sum \mathcal{A}^{kl} \quad (2)$$

where $\mathcal{E}(k, l)$ represents the average connection between two VE-Regions k and l ; n_{kl} is the total number of connections between nodes in VE-Regions k and l .

We assess the significant difference between CG and GG in connections between/within each VE-Region in the group average brain networks using Mann–Whitney U test, as illustrated in Equation 3.

$$[P_{kl}, zval_{kl}] = U[\text{vec}(\mathcal{A}_C^{kl}), \text{vec}(\mathcal{A}_G^{kl})] \quad (3)$$

Here, \mathcal{A}_C^{kl} represents the connections between VE-Regions k and l of average CG brain network, while \mathcal{A}_G^{kl} represents the connections between VE-Regions k and l of average GG brain network. \mathcal{A}_C^{kl} and \mathcal{A}_G^{kl} are then converted to vectors for Mann–Whitney U test. P_{kl} denotes the probability of the difference between CG and GG in connections between VE-Regions k and l , with lower values (typically $P_{kl} \leq 0.05$) indicating a more significant difference; $zval_{kl}$ denotes the value of the normal statistic between CG and GG in connections between/within VE-Regions k and l , with larger absolute values (typically $zval_{kl} \geq 1.96$ corresponding to $P_{kl} \leq 0.05$) indicating a more significant difference. Negative $zval$ indicates smaller values in the first group, while positive $zval$ indicates larger values. However, the interpretation of $zval_{kl}$ is limited here because \mathcal{A}_C^{kl} and \mathcal{A}_G^{kl} contain negative values, making the $zval_{kl}$ statistic less meaningful.

- **Analysis of group average brain networks across different density.**

We analyze the effects of density on brain networks using the MST (Van Wijk et al., 2010) to ensure that all graphs of different densities are node-connected. An MST is a subgraph that connects all nodes using exactly $R - 1$ edges, where R is the number of nodes in the network. We first find the MST and

then add edges to ensure the graph is node-connected. The connection density p refers to the proportion of edges presented in the network relative to the total possible edges ($(R - 1)R/2$, where $R = 308$). Notably, when computing MST graphs for MSNs, negative values are treated as 0.

We denote \mathcal{M}_p as the MST network with connection density p of a brain network \mathcal{A} . Given that an MST network \mathcal{M}_p is node-connected, the minimum connection density p of MST network is $(R - 1)/[(R - 1)R/2] = 0.0065$, where $R = 308$. In this study, connection densities used are: $p \in \{0.0065, 0.01, 0.05, 0.1, 0.15, 0.2, 0.25, 0.3, 0.35, 0.4, 0.5, 0.6, 0.7, 0.8, 0.9, 1\}$.

For a MST brain network \mathcal{M}_p , we extract the nonzero values from upper triangle elements of \mathcal{M}_p , denoted as t_p , as shown in Equation 4.

$$t_p = \text{vec}(\mathcal{M}_p(i, j) \mid 1 \leq i < j \leq R \text{ and } \mathcal{M}_p(i, j) \neq 0) \quad (4)$$

We denote t_p^C and t_p^G as the nonzero values of upper triangle elements of the CG and GG average brain networks with connection density p , respectively.

Then, the Mann–Whitney U test is used to evaluate the significant difference between t_p^C and t_p^G , as shown in Equation 5.

$$[P_p, zval_p] = U(t_p^G, t_p^C) \quad (5)$$

P_p denotes the probability of the difference between t_p^G and t_p^C for specific p ; $zval_p$ denotes the value of the normal statistic between t_p^G and t_p^C .

- **Nodal topological features in group networks across different network densities.**

Eight nodal topological features are adopted to characterize the nodal topological organization of brain networks. Each nodal topological feature is a vector with a length equivalent to the number of regions, which is $R = 308$ in this study.

1. The **node degree** $F_{nd}(i)$ refers to the number of connections that node i has to other nodes in a graph.
2. The node strength $F_{ns}(i)$ is the sum of connection weights for node i .
3. The **eigenvector centrality** (Newman, 2010) of node i , $F_{ec}(i)$, is equivalent to the i -th element in the eigenvector corresponding to the largest eigenvalue of the adjacency matrix.
4. The **participation coefficient** $F_{pc}(i)$ (Guimera and Nunes Amaral, 2005) quantifies how the connections of node i are distributed across various modules by representing the proportion of its connectivity allocated to each module, identified here using the Louvain community detection algorithm (Blondel et al., 2008).
5. The **node centrality** $F_{nc}(i)$ (Brandes, 2001) quantifies the proportion of shortest paths between all node pairs in the network that pass through a given index node i .
6. The **local efficiency** F_{le} (Rubinov and Sporns, 2010) represents the global efficiency calculated within each node's neighborhood and is associated with the clustering coefficient.
7. The **(weighted) clustering coefficient** F_{cc} (Onnela et al., 2005) is defined as the average "intensity" (geometric mean) of all triangles associated with each node.
8. The **nodal versatility** $F_{mv}(i)$ (Shinn et al., 2017) assesses the consistency with which a node i in a modular decomposition is linked to a particular module. The identification of modules in this research is derived by the Louvain community detection algorithm (Blondel et al., 2008)).

For analyzing the nodal topological features of group networks, the Euclidean distance is utilized to quantify the disparity between CG and GG average networks across each nodal topological feature at different densities p . Prior to computing the Euclidean distance, each feature of the two groups is normalized to $[0, 1]$ with the Min-Max method across all p values. We use $D_V(p)$ represents Euclidean distance for a specific type of nodal topological feature $V \in \{nd, ns, ec, pc, nc, le, cc, nv\}$ at a given connection density p .

- **Intra-/Inter-modular analysis based on VE-Regions for the group brain networks.**

We identify all intra-VE and inter-VE connections within a brain network \mathcal{A} , denoted as \mathcal{A}^{intra} and \mathcal{A}^{inter} , respectively. Furthermore, we compare the strength of intra-VE connections ($S_{intra} =$

$\sum \mathcal{A}_p^{kl}, k = l$) and inter-VE connections ($S_{inter} = \sum \mathcal{A}_p^{kl}, k \neq l$) for CG and GG at a specific connection density ($p = 0.1$) processed by MST, with all connections positive.

- **Intra-/Inter-hemispheric analysis for the group brain networks.**

For a brain network \mathcal{A} , we obtain the intra-hemispheric connections in left hemisphere (LL) and right hemisphere (RR), as well as inter-hemispheric correlations between left and right hemisphere (LR), which can be denoted as \mathcal{A}^{LL} , \mathcal{A}^{RR} and \mathcal{A}^{LR} , respectively. Moreover, we compare the strength of left intra-hemispheric connections ($S_{LL} = \sum \mathcal{A}_p^{LL}$), right intra-hemispheric connections ($S_{RR} = \sum \mathcal{A}_p^{RR}$) and inter-hemispheric correlations ($S_{LR} = \sum \mathcal{A}_p^{LR}$) for CG and GG at a specific connection density ($p = 0.1$) processed by MST, with all connections positive.

2.2.3 Individual Cognitive Analyses for MSNs

This part explores the relationship between cognitive performance and the structural organization of brain networks, using two analytical approaches: the connection strengths between VE-Regions and the global topological features of brain networks. Both analyses rely on the Spearman correlation to quantify the associations between network metrics and full-scale IQ scores.

The Spearman correlation is a non-parametric measure of rank correlation, evaluating the statistical dependence between the rankings of two variables. It determines how well the relationship between two variables can be described using a monotonic function. The Spearman correlation coefficient (SCC) is denoted as ρ in this work. We consider $\rho > 0.2$ as indicating a significant positive monotonic relationship, while $\rho < -0.2$ is interpreted as a significant negative monotonic relationship.

The following in this part focuses on individual cognitive analysis based on VE-Region connections and global topological features of brain networks.

- **Individual cognitive analysis based on VE-Regions.**

As defined in 2.2.2, $\mathcal{E}(k, l)$ represents the VE connection strength between two VE-Regions k and l within a brain network \mathcal{A} . We introduce $E^p(k, l)$ as the vector of the connection strength between the two VE-Regions k and l across all subjects' brain networks at connection density p . To measure the relationship between VE connections and cognitive performance, we use $\rho^p(E^p(k, l), C)$ to denote the SCCs between each VE-Region connection strength $E^p(k, l)$ and full-scale IQ scores C .

- **Individual cognitive analysis with global topological features of brain networks.**

Ten network metrics are adopted to characterize the global topological organization of structural brain networks:

1. The **assortativity** (Newman, 2002) f_a is defined as the correlation coefficient for the degrees of neighboring nodes, which refers to the tendency of nodes in a network to link with other similar nodes.
2. The **transitivity** f_t is the ratio of “triangles to triplets” in the network.
3. A network’s **global efficiency** (Latora and Marchiori, 2001) f_{ge} is the reciprocal of the harmonic mean of its path lengths.
4. The **characteristic path length** (Watts and Strogatz, 1998) f_{cpl} is the average shortest path length between all possible pairs of nodes in a network. Moreover, the characteristic path length of a network is strongly positively correlated with the network’s average strength.
5. The **mean participation coefficient** f_{mpc} can measure the global integration of a network.
6. The **mean clustering coefficient** f_{mcc} is the mean value of the clustering coefficient of a network.
7. The **mean versatility** f_{mv} is the mean value of nodal versatility which can measure the global integration of a network.
8. The **ratio of left to right intra-hemispheric connections** is denoted as $f_{lr} = \frac{\sum \mathcal{A}_p^{LL}}{\sum \mathcal{A}_p^{RR}}$, where \mathcal{A}_p^{LL} and \mathcal{A}_p^{RR} are denoted as the intra-hemispheric connections in the left and right hemisphere of a MST network with density p , respectively.
9. The **ratio of intra- to inter-hemispheric connections** is denoted as $f_{ii} = \frac{\sum \mathcal{A}_p^{LL} + \sum \mathcal{A}_p^{RR}}{\sum \mathcal{A}_p^{LR}}$, where \mathcal{A}_p^{LR} is denoted as the inter-hemispheric connections of a MST network with density p .
10. The **ratio of intra- to inter-VE connections** is denoted as $f_{VE} = \frac{\sum \mathcal{A}_p^{kl}, k=l}{\sum \mathcal{A}_p^{kl}, k \neq l}$, where \mathcal{A}_p^{kl} represents connections between two VE-Regions k and l in a MST network with density p .

In this research, we aim to enhance our comprehension of the relationship between these topological features and cognitive abilities. We analyze Spearman correlations between the full-scale IQ scores and each global topological feature of the brain networks.

Here we utilize $\rho^p(f_v^p, C)$ to denote the SCC between each global topological feature f_v^p and full-scale IQ scores C , where

$v \in \{a, t, ge, cpl, mpc, mcc, mv, lr, ii, VE\}$ represents various global topological features.

3 RESULTS

3.1 Group Analysis Results for MSNs

As illustrated in Section 2.2.2, we conducted group comparison analyses of MSNs, and the results are shown in Fig. 2.

3.1.1 Results of VE-Region Analysis for Group Average Brain Networks

- **Heatmap Comparison for Group Average Brain Networks.**

Fig. 2 a shows the heatmaps of group average networks for VE-ordered MSNs. In each heatmap, the value range represented by colors varies from -1 to 1, and warmer colors indicate higher values. Typically, MSNs encompass both positive and negative values. Notably, it appears that there is no discernible visual distinction between the CG and GG in the heatmaps of the group average MSNs.

- **Comparison of Top 1% Group Brain Networks.**

Fig. 2 b displays the top 1% (absolute) of group average brain networks, as visualized using Brain-Net Viewer (Xia et al., 2013). The seven-colored nodes represent the grouped VE-Regions, and the color links denote intra-VE connections, while grey links denote inter-VE connections. The size of nodes reflects the degree in the network. Top 1% of a brain network ($R = 308$) contains $[(R - 1)R/2] \times 1\% = 474$ connections. Notably, discernible visual differences exist between the CG and GG average MSNs for the top 1% of connections: GG shows more intra-VE connections and fewer inter-VE connections compared to CG.

- **Results of Average VE-Region Connections of Group Brain Networks.**

As detailed in Section 2.2.2, we compute the average VE connection \mathcal{E} , for the average brain network of each group. The results are shown in Figure 2 c. In the figure, each cell in the heatmaps represents the average connection between VE-Regions k and l , denoted as $\mathcal{E}(k, l)$. The seven diagonal values correspond to the average of connections within each intra-VE-Region, while the values in the lower triangle represent the average of connection between each inter-VE-Region pair. From the visualization, the group

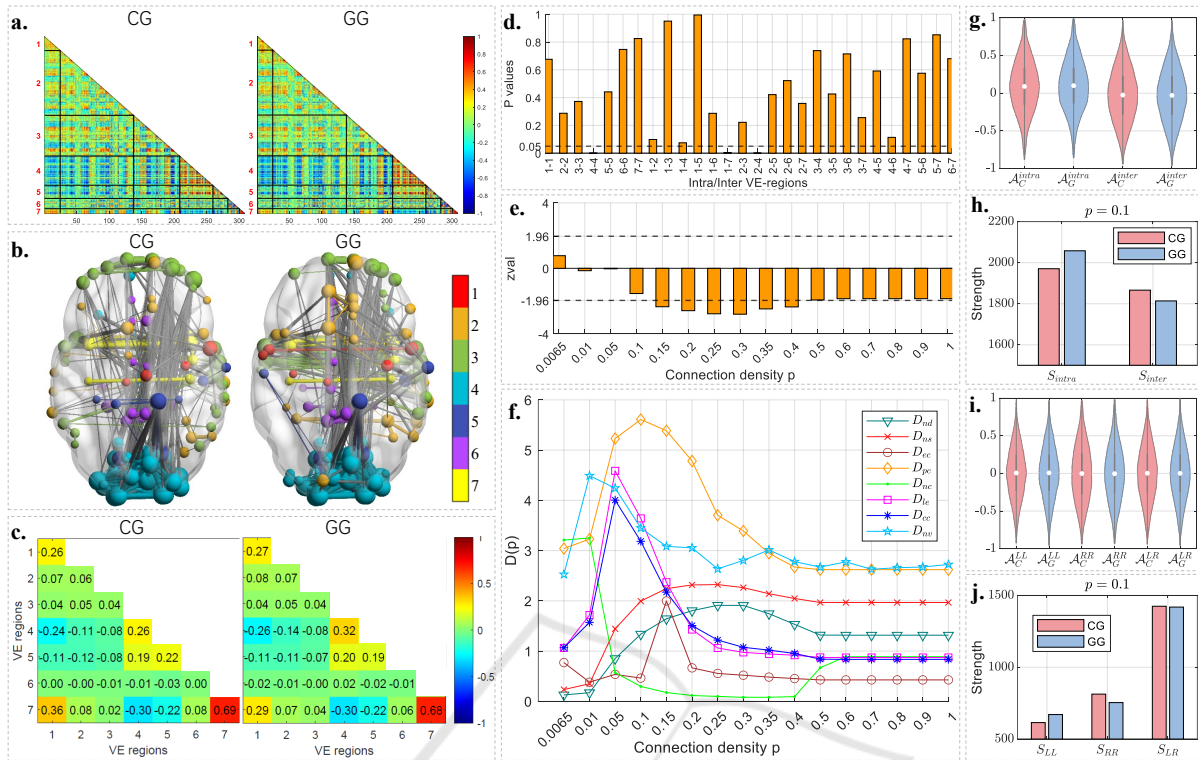


Figure 2: Comparison of CG and GG average brain networks. **a.** Heatmaps of the CG (left) and GG (right) average networks, organized by the seven VE-Regions. **b.** Comparison of the top 1% (absolute) of CG (left) and GG (right) average brain networks, labeled with seven VE-Regions. **c.** Average VE-Region connection \mathcal{E} of each group average brain network. **d.** P values of the Mann–Whitney U test for CG and GG across each VE-Region. **e.** $zval_p$ results of the Mann–Whitney U test between t_p^C and t_p^G for group average MSNs across different connection densities p . **f.** Euclidean distance between CG and GG average networks on each nodal topological feature across different connection densities p . **g.** Violins for intra-/inter-VE connections of group average MSNs. **h.** Strength of intra-VE (S_{intra}) and inter-VE (S_{inter}) connections for CG and GG at a connection density of $p = 0.1$. **i.** Violins for intra-/inter-hemispheric connections of group average MSNs. **j.** Strengths of hemispheric connections, S_{LL} , S_{RR} and S_{LR} , at a connection density of $p = 0.1$.

average MSNs reveal more pronounced differences between the CG and GG in the average VE-Region connections in VE 4-4, 4-6, 5-5, 1-7 and 2-4 (differences ≥ 0.3). Specifically, GG exhibits stronger average connections in VE 4-4 and 4-6, while showing weaker average connections in VE 5-5, 1-7 and 2-4.

- **Significant Difference Evaluation Between CG and GG Across Each VE-Region Connections.**

As described in Section 2.2.2, we evaluate the significant difference between the connections of \mathcal{A}_C^{kl} and \mathcal{A}_G^{kl} for each VE- k and VE- l . Figure 2 **d** provide a visual representation of P_{kl} values resulting from the Mann–Whitney U test. It is apparent that the group average MSNs exhibit significant differences between the CG and GG in the VE connections 4-4, 1-7 and 2-4, with $P_{kl} < 0.05$. Additionally, notable differences are observed in VE connections 1-2, 1-4 and 4-6, with $P_{kl} \gtrsim 0.05$. These findings align closely with the “Results of average VE-Region connections of group brain networks,” which also identify pronounced dif-

ferences between CG and GG in VE-Region connections 4-4, 4-6, 1-7 and 2-4 (differences ≥ 0.3).

3.1.2 Analysis Results of Group Average Brain Networks Across Different Density

As described in Section 2.2.2, we conducted an analysis to examine the effects of network density on the difference between average CG and GG brain networks by comparing t_p^C and t_p^G across different connection densities p . Fig. 2 **e** displays the $zval_p$ results of the Mann–Whitney U test between t_p^C and t_p^G for group average MSNs across different connection densities p . The $zval_p$ values for MSN exceed 1.96 for p values ranging from 0.15 to 0.4, reaching a maximum of 2.80 at $p = 0.3$, indicating significantly larger connection values in the CG average MSN compared to the GG average MSN. Notably, the $zval_p$ values stabilize as $p \geq 0.5$. This stability arises from the roughly equal numbers of positive and negative connections in the MSNs, as observed in Section 3.1.4, with negative

connections being treated as zero. This also explains the stability observed in the nodal topological feature analysis when $p \geq 0.5$ in the following Section 3.1.3.

3.1.3 Analysis Results of Nodal Topological Features in Group Networks Across Various Network Densities

Figure 2 f presents the Euclidean distance $D_V(p)$ between the CG and GG average networks on each nodal topological feature at different densities p , including: D_{nd} (teal triangles), D_{ns} (red crosses), D_{ec} (red circles), D_{pc} (orange diamonds), D_{nc} (green dots), D_{le} (purple squares), D_{cc} (blue asterisks), D_{pc} (cyan stars).

Notably, the trends of D_{nd} vs. D_{ns} and D_{cc} vs. D_{le} exhibit similar patterns as p varies. Additionally, the values of D_{ns} and D_{le} are slightly higher than those of D_{nd} and D_{cc} , respectively. The details are as follows:

- Both D_{nd} and D_{ns} values start low at very small p and show a slight increase as p increases, with a relatively stable trend as $p = 0.15 \sim 0.3$.
- Both D_{le} and D_{cc} values start low, rise sharply, peak at $p = 0.05$, and then decrease rapidly.
- D_{pc} values exhibit an early sharp increase, peaking at $p = 0.1$, followed by a gradual decline. Despite the decline, they maintain higher values compared to other features.
- D_{mv} values start high, peak early ($p = 0.01$), and then decline steadily as density increases, still maintaining higher values compared to other features.
- D_{nc} values show an initial peak at lower densities ($p = 0.0065$ and $p = 0.01$), followed by a rapid decline, stabilizing at very low values.
- D_{ec} remain very low values except for a noticeable increase at $p = 0.15$.

3.1.4 Results of Intra-/Inter-modular Connections Based on VE-Regions for Group Brain Networks

Figure 2 g shows violin plots representing the intra-VE and inter-VE connections for CG and GG average MSNs. Each violin includes a white dot representing the average value. The light red violins correspond to \mathcal{A}_C^{intra} and \mathcal{A}_C^{inter} for CG, while the light blue violins represent \mathcal{A}_G^{intra} and \mathcal{A}_G^{inter} for GG. The connection values in the group average MSNs range from -1 to 1 . Moreover, the average value of intra-VE connections is consistently higher than that of inter-VE connections in both CG and GG average MSNs. However, the differences in intra-VE and inter-VE connec-

tions between CG and GG are minimal in the original group average MSNs.

Fig. 2 h illustrates the intra-VE connection strength (S_{intra}) and inter-VE connection strength (S_{inter}) for CG and GG at a connection density of $p = 0.1$. Both CG and GG exhibit stronger intra-VE connectivity compared to inter-VE connectivity. However, GG demonstrates stronger intra-VE connectivity and weaker inter-VE connectivity compared to CG.

3.1.5 Results of Intra-/Inter-hemispheric Analysis for Group Average Brain Networks

Fig. 2 i illustrates the violin plots depicting the intra-/inter-hemispheric connections of each group average brain network. The dot in each violin represents the average value. The light red violins represent the LL, RR, and LR connections in the average CG brain network, while the light blue violins represent those in the average GG brain network. It can be observed that the differences in hemispheric connections between CG and GG are minimal in the original group average MSNs.

Fig. 2 j illustrates the hemispheric connection strengths, S_{LL} , S_{RR} , and S_{LR} , at a connection density of $p = 0.1$. The results show that both CG and GG exhibit stronger right intra-hemispheric connections than left intra-hemispheric connections, and stronger inter-hemispheric connections than intra-hemispheric ones. However, GG shows higher S_{LL} , weaker S_{RR} , and slightly weaker S_{LR} compared to CG.

3.2 Results of Individual Cognitive Analysis for MSNs

As outlined in Section 2.2.3, we analyzed the relationship between cognitive performance and the structural organization of individual MSNs using Spearman correlation, with the results presented in Fig. 3. As stated in Section 3.1, stability in MSNs occurs when the connection density $p \geq 0.5$. Therefore, our analysis focuses on connection densities $p \leq 0.6$ in this section.

3.2.1 Results of Individual Cognitive Analysis Based on VE-Regions

As described in 2.2.3, we analyzed the Spearman correlations between full-scale IQ scores and each VE-Region connection strength $E^p(k,l)$ across different connection densities p . The SCC results $\rho^p(E^p(k,l), C)$ are shown in Fig. 3 a. Each line corresponds to a different connection density $p = 0.0065 \sim$

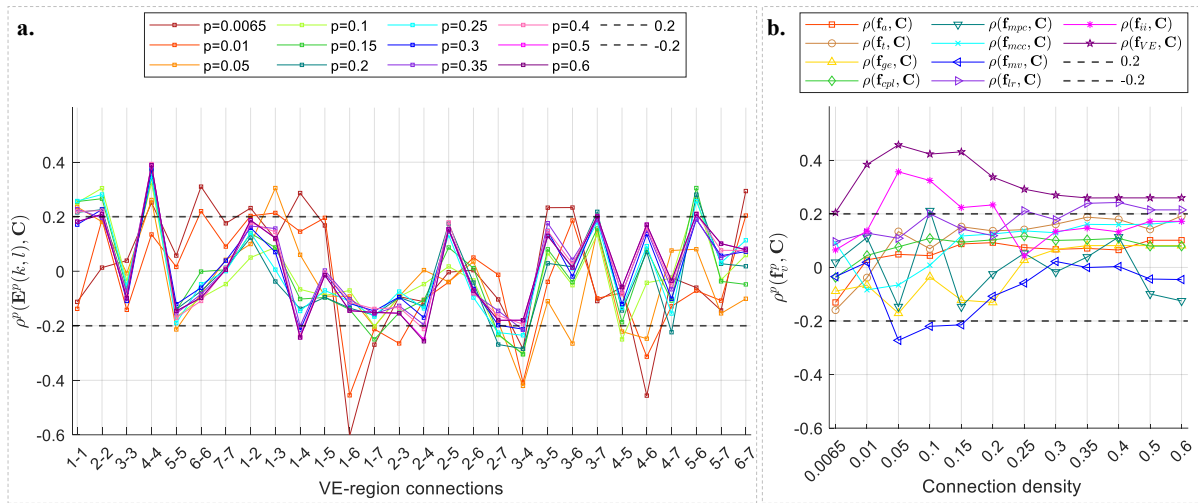


Figure 3: Results of individual cognitive analysis for MSNs. **a.** SCCs $\rho^p(E^p(k,l), C)$ between each VE-Region connection strength $E^p(k,l)$ and full-scale IQ scores across different connection densities p . **b.** SCCs $\rho^p(f_v^p, C)$ between various global topological features (v) of MSNs and full-scale IQ scores (C) across different connection densities p .

0.6. The x-axis represents the various VE-Region connections, while the y-axis denotes the SCC values. It can be observed that:

- For lower connection densities ($p \leq 0.05$), SCCs exhibit more pronounced variations and instability compared to those observed at higher connection densities ($p \geq 0.1$) for the corresponding VE-Region connections, particularly in 1-1, 6-6, 1-4, 1-6, 3-6 and 4-6. However, there are higher SCCs in VE-Region connections of 1-6, 3-4, and 4-6 as $p \leq 0.05$.
- As the connection density $p \geq 0.1$, the SCCs for each VE-Region connection tend to stabilize, with significant positive correlations for VE-Region connections 1-1, 2-2, 4-4, 3-7, 5-6, 1-2 and 4-6, significant negative correlations for VE-Region connections 5-5, 1-4, 1-7, 2-4, 2-7, 3-4, 4-5 and 4-7.

3.2.2 Results of Individual Cognitive Analysis with Global Topological Features

As described in 2.2.3, we analyzed the Spearman correlations between each global topological feature of brain networks and the full-scale IQ scores across different connection densities p . The results are displayed in Fig. 3 b. The x-axis represents different values of p from 0.0065 to 1, while the y-axis shows the SCCs for each feature. It can be observed that the values of $\rho^p(f_v^p, C)$ vary with different global topological features for MSNs:

- IQ is significantly positively correlated with the ratio of intra- to inter-hemispheric connections (f_{ii}) for $0.05 \leq p \leq 0.2$ (with the highest $\rho = 0.36$

at $p = 0.05$), and with the ratio of intra- to inter-VE connections (f_{VE}) across all p values (with the highest $\rho = 0.46$ at $p = 0.05$). These findings suggest that individuals with higher IQ tend to exhibit stronger intra-hemispheric and intra-modular connections while displaying weaker inter-hemispheric and inter-modular connections.

- IQ is significantly positively correlated with ratio of left to right intra-hemispheric connections f_{lr} when $p = 0.1$, indicating stronger left intra-hemispheric connections in individuals with higher IQ.
- IQ is significantly negatively correlated with mean versatility f_{mv} when $0.05 \leq p \leq 0.15$, suggesting less versatility in MSNs of individuals with high cognitive performance.
- Correlations between IQ and mean participation coefficient f_{mpc} exhibit sharp fluctuations as connection density p changes for MSNs.
- There are no significant correlations between IQ and other global topological features, including assortativity f_a , transitivity f_t , global efficiency f_{ge} , characteristic path length f_{cpl} (average strength), mean weighted clustering coefficient f_{mcc} .
- Generally, the correlations $\rho^p(f_v^p, C)$ tend to achieve higher values when $0.05 \leq p \leq 0.15$ in more cases.

4 DISCUSSION

In this study, we used sMRI data to compute the MSNs of children with different intelligence levels. We compared group-level MSNs of CG and GG to identify key differences and analyzed individual-level data to link cognitive performance with brain network structure. The results of our experiments revealed several important findings:

- **The effects of connection density.**

The effects of connection density on brain networks reveal distinct trends in both group and individual analyses. **(1) Group-level analysis:** The significant differences between the CG and GG networks become more pronounced when $p = 0.15 \sim 0.4$. The Euclidean distances between the nodal topological features of two groups show high sensitivity to changes in density when $p \leq 0.05$, peaking between $p = 0.05 \sim 0.25$ in most cases. **(2) Individual-level analysis:** For VE-Region connections, lower connection densities ($p \leq 0.05$) tend to show more pronounced variations in correlations with IQ, while higher densities stabilize these correlations. For global topological features, higher SCCs are achieved when $p = 0.05 \sim 0.15$. Generally, a connection density of $p = 0.05 \sim 0.15$ is recommended in MSN cognitive analysis for stable and optimal results. Thus, we chose a connection density of $p = 0.1$ for group-level analyses of intra-/inter-modular and intra-/inter-hemispheric connections.

- **The relationship between VE-Region (modular) connections and cognitive performance.**

Both the group and individual analyses reveal that there are stronger connections in VE 4-4 (secondary sensory area), 1-2 (motor to association area) and 4-6 (secondary sensory to limbic area) for individuals with higher IQ scores. Conversely, weaker connections in VE 1-7 (motor to insular area), 2-4 (association to secondary sensory area) and 1-4 (motor to secondary sensory area) are observed in individuals with higher IQ scores. These findings suggest that higher cognitive performance is linked not only to enhanced connectivity in specific sensory, motor, and limbic areas but also to a selective reduction in certain modular connections, potentially contributing to greater neural efficiency.

- **Analyses on intra-/inter-modular and intra-/inter-hemispheric connections**

In the group average analysis, both CG and GG demonstrate stronger intra-VE connections compared to inter-VE connections, as well as stronger right intra-hemispheric connections compared to left intra-hemispheric connections, aligning with (Jiang et al.,

2019). Moreover, both group and individual analyses reveal that individuals with higher IQ tend to display stronger intra-VE and intra-hemispheric connections, alongside weaker inter-VE and inter-hemispheric connections. As stronger MSN connectivity reflects greater morphometric similarity, individuals with higher IQ demonstrate higher morphometric similarity within VE-Regions and hemispheres, alongside greater differentiation between VE-Regions and between the left and right hemispheres. These findings suggest a more integrated intra-hemispheric and intra-VE-Region organization, which may facilitate more efficient cognitive processing (Solé-Casals et al., 2019; Santarnecchi et al., 2015; Krupnik et al., 2021). Additionally, the analysis shows that a higher ratio of left-to-right intra-hemispheric connections in MSNs is associated with enhanced IQ, suggesting that individuals with higher IQ exhibit a more balanced distribution of connections between the left and right intra-hemispheric networks. Interestingly, this finding contrasts with (Solé-Casals et al., 2019), which reported stronger right intra-hemispheric connections for the GG in traditional SCNs.

- **The relationship between topological features and cognitive performance.**

Our analysis reveals significant associations between certain topological features of brain networks and IQ. **(1) Group-level analysis:** Sensitivity to connection density varies across nodal topological features. The participation coefficient F_{pc} , nodal versatility F_{nv} , local efficiency F_{le} and clustering coefficient f_{cc} are sensitive to density variations, and achieve higher Euclidean distance when $p = 0.05 \sim 0.1$. Both the node degree F_{nd} and node strength F_{ns} stably achieve high Euclidean distance as $p = 0.15 \sim 0.3$. However, the node centrality F_{nc} and eigenvector centrality F_{ec} show little utility for cognitive analysis, as they do not perform well in distinguishing cognitive groups. **(2) Individual-level analyses:** IQ is negatively correlated with mean versatility f_{mv} at $p = 0.05 \sim 0.1$, contrasting with (Solé-Casals et al., 2019), which found higher mean versatility for the GG in traditional SCNs. Other features, such as the mean participation coefficient, show fluctuating correlations across densities are less reliable for MSN cognitive analysis.

This study has some limitations. First, the small sample size may reduce the generalizability of the findings, underscoring the need for larger cohorts in future research. Second, we neglect the negative value in MSNs in connection density related analyses, potentially affecting the interpretation of network structures. Third, while the study focuses on structural networks, integrating functional imaging data could

provide deeper physiological and cognitive insights.

5 CONCLUSIONS

In this study, we constructed MSNs from sMRI data to investigate brain network characteristics in children with different intelligence levels. Group-level analyses were performed by comparing the average MSNs of the CG and GG to identify key differences in brain network topology. Additionally, we conducted individual-level analyses to explore the relationship between cognitive performance and the structural organization of brain networks.

Our results show that variations in connection density have a significant impact on both global and nodal topological features, with each exhibiting distinct trends. A connection density of $p = 0.05 \sim 0.15$ is recommended in MSN cognitive analysis for stable and optimal results. Additionally, gifted individuals exhibit stronger intra-hemispheric and intra-modular connectivity, weaker inter-hemispheric and inter-modular connectivity, a more balanced distribution of left-to-right intra-hemispheric connections, and lower mean versatility, which may be associated with more efficient and stable cognitive processing. Moreover, the analyses on anatomical modularity of VE indicate that higher cognitive performance is linked not only to enhanced connectivity in specific modules (such as secondary sensory area, motor to association area, and secondary sensory to limbic area) but also to a selective reduction in certain modular connections (such as motor to insular area, association to secondary sensory area, and motor to secondary sensory area), potentially contributing to greater neural efficiency. Furthermore, key topological features, such as participation coefficient, nodal versatility, local efficiency and clustering coefficient, are linked to cognitive performance at specific connection density. However, other features, such as the mean participation coefficient (showing fluctuating correlations across densities), assortativity, characteristic path length, and the mean weighted clustering coefficient (showing no significant correlations with IQ), are less reliable for MSN cognitive analysis.

In conclusion, our findings highlight the effects of connection density and demonstrate how modular and hemispheric connectivity, along with specific topological features, relate to children's cognitive performance. These insights pave the way for future research to further explore the neural mechanisms underlying cognitive abilities with brain networks. By using larger, more diverse samples and longitudinal designs, future studies could enhance our understand-

ing of how brain network topology evolves with cognitive development and deepen our knowledge of the neural mechanisms that underpin human intelligence.

ACKNOWLEDGEMENTS

This work was carried out as part of the doctoral program in Experimental Sciences and Technology at the University of Vic - Central University of Catalonia. F.D. work was partially supported by the National Natural Science Foundation of China (Key Program) (No. 11932013), and the Tianjin Science and Technology Plan Project (No. 22PTZWHZ00040). C.F.C work was partially supported by grants PICT 2020-SERIEA-00457 and PIP 112202101 00284CO (Argentina).

REFERENCES

- Blondel, V. D., Guillaume, J.-L., Lambiotte, R., and Lefebvre, E. (2008). Fast unfolding of communities in large networks. *Journal of statistical mechanics: theory and experiment*, 2008(10):P10008.
- Brandes, U. (2001). A faster algorithm for betweenness centrality. *Journal of mathematical sociology*, 25(2):163–177.
- Desikan, R. S., Ségonne, F., Fischl, B., Quinn, B. T., Dickerson, B. C., Blacker, D., Buckner, R. L., Dale, A. M., Maguire, R. P., Hyman, B. T., et al. (2006). An automated labeling system for subdividing the human cerebral cortex on mri scans into gyral based regions of interest. *Neuroimage*, 31(3):968–980.
- Faskowitz, J., Betzel, R. F., and Sporns, O. (2022). Edges in brain networks: Contributions to models of structure and function. *Network Neuroscience*, 6(1):1–28.
- Fischl, B. and Dale, A. M. (2000). Measuring the thickness of the human cerebral cortex from magnetic resonance images. *Proceedings of the National Academy of Sciences*, 97(20):11050–11055.
- Genon, S., Eickhoff, S. B., and Kharabian, S. (2022). Linking interindividual variability in brain structure to behaviour. *Nature Reviews Neuroscience*, 23(5):307–318.
- Ghosh, S. S., Kakunoori, S., Augustinack, J., Nieto-Castanon, A., Kovelman, I., Gaab, N., Christodoulou, J. A., Triantafyllou, C., Gabrieli, J. D., and Fischl, B. (2010). Evaluating the validity of volume-based and surface-based brain image registration for developmental cognitive neuroscience studies in children 4 to 11 years of age. *Neuroimage*, 53(1):85–93.
- Guimera, R. and Nunes Amaral, L. A. (2005). Functional cartography of complex metabolic networks. *nature*, 433(7028):895–900.
- Heinsfeld, A. S., Franco, A. R., Craddock, R. C., Buchweitz, A., and Meneguzzi, F. (2018). Identification of

- autism spectrum disorder using deep learning and the ABIDE dataset. *NeuroImage: Clinical*, 17:16–23.
- Jiang, X., Shen, Y., Yao, J., Zhang, L., Xu, L., Feng, R., Cai, L., Liu, J., Chen, W., and Wang, J. (2019). Connectome analysis of functional and structural hemispheric brain networks in major depressive disorder. *Translational psychiatry*, 9(1):136.
- Kong, X.-z., Liu, Z., Huang, L., Wang, X., Yang, Z., Zhou, G., Zhen, Z., and Liu, J. (2015). Mapping individual brain networks using statistical similarity in regional morphology from mri. *PLoS one*, 10(11):e0141840.
- Krupnik, R., Yovel, Y., and Assaf, Y. (2021). Inner hemispheric and interhemispheric connectivity balance in the human brain. *Journal of Neuroscience*, 41(40):8351–8361.
- Latora, V. and Marchiori, M. (2001). Efficient behavior of small-world networks. *Physical review letters*, 87(19):198701.
- Li, J., Seidlitz, J., Suckling, J., Fan, F., Ji, G.-J., Meng, Y., Yang, S., Wang, K., Qiu, J., Chen, H., et al. (2021). Cortical structural differences in major depressive disorder correlate with cell type-specific transcriptional signatures. *Nature communications*, 12(1):1647.
- Li, W., Yang, C., Shi, F., Wu, S., Wang, Q., Nie, Y., and Zhang, X. (2017). Construction of individual morphological brain networks with multiple morphometric features. *Frontiers in Neuroanatomy*, 11:34.
- Lo, C.-Y. Z., He, Y., and Lin, C.-P. (2011). Graph theoretical analysis of human brain structural networks. *Reviews in the Neurosciences*, 22(5):551–563.
- Newman, M. (2010). *Networks: An Introduction*. Oxford University Press.
- Newman, M. E. (2002). Assortative mixing in networks. *Physical review letters*, 89(20):208701.
- Onnela, J.-P., Saramäki, J., Kertész, J., and Kaski, K. (2005). Intensity and coherence of motifs in weighted complex networks. *Physical Review E—Statistical, Nonlinear, and Soft Matter Physics*, 71(6):065103.
- Park, H.-J. and Friston, K. (2013). Structural and functional brain networks: from connections to cognition. *Science*, 342(6158):1238411.
- Rubinov, M. and Sporns, O. (2010). Complex network measures of brain connectivity: uses and interpretations. *Neuroimage*, 52(3):1059–1069.
- Santarnecchi, E., Tatti, E., Rossi, S., Serino, V., and Rossi, A. (2015). Intelligence-related differences in the asymmetry of spontaneous cerebral activity. *Human brain mapping*, 36(9):3586–3602.
- Sebenius, I., Seidlitz, J., Warrier, V., Bethlehem, R. A., Alexander-Bloch, A., Mallard, T. T., Garcia, R. R., Bullmore, E. T., and Morgan, S. E. (2023). Robust estimation of cortical similarity networks from brain mri. *Nature Neuroscience*, 26(8):1461–1471.
- Seidlitz, J., Váša, F., Shinn, M., Romero-Garcia, R., Whitaker, K. J., Vértes, P. E., Wágstyl, K., Reardon, P. K., Clasen, L., Liu, S., et al. (2018). Morphometric similarity networks detect microscale cortical organization and predict inter-individual cognitive variation. *Neuron*, 97(1):231–247.
- Shinn, M., Romero-Garcia, R., Seidlitz, J., Váša, F., Vértes, P. E., and Bullmore, E. (2017). Versatility of nodal affiliation to communities. *Scientific Reports*, 7(1):4273.
- Solé-Casals, J., Serra-Grabulosa, J. M., Romero-Garcia, R., Vilaseca, G., Adan, A., Vilaró, N., Bargalló, N., and Bullmore, E. T. (2019). Structural brain network of gifted children has a more integrated and versatile topology. *Brain Structure and Function*, 224(7):2373–2383.
- Sun, K., Chen, G., Liu, C., Chu, Z., Huang, L., Li, Z., Zhong, S., Ye, X., Zhang, Y., Jia, Y., et al. (2024a). A novel msn-ii feature extracted from t1-weighted mri for discriminating between bd patients and mdd patients. *Journal of Affective Disorders*.
- Sun, Y., Chen, P., Liu, Y., and Zhao, K. (2024b). Macroscale brain structural network coupling is related to ad progression. In *2024 IEEE International Symposium on Biomedical Imaging (ISBI)*, pages 1–4. IEEE.
- Sun, Y., Lee, R., Chen, Y., Collinson, S., Thakor, N., Bezirianos, A., and Sim, K. (2015). Progressive gender differences of structural brain networks in healthy adults: a longitudinal, diffusion tensor imaging study. *PLoS one*, 10(3):e0118857.
- Van Wijk, B. C., Stam, C. J., and Daffertshofer, A. (2010). Comparing brain networks of different size and connectivity density using graph theory. *PLoS one*, 5(10):e13701.
- Váša, F., Seidlitz, J., Romero-Garcia, R., Whitaker, K. J., Rosenthal, G., Vértes, P. E., Shinn, M., Alexander-Bloch, A., Fonagy, P., Dolan, R. J., et al. (2018). Adolescent tuning of association cortex in human structural brain networks. *Cerebral Cortex*, 28(1):281–294.
- Vértes, P. E., Rittman, T., Whitaker, K. J., Romero-Garcia, R., Váša, F., Kitzbichler, M. G., Wágstyl, K., Fonagy, P., Dolan, R. J., Jones, P. B., et al. (2016). Gene transcription profiles associated with inter-modular hubs and connection distance in human functional magnetic resonance imaging networks. *Philosophical Transactions of the Royal Society B: Biological Sciences*, 371(1705):20150362.
- Von Economo, C. (1929). *The cytoarchitectonics of the human cerebral cortex*. H. Milford Oxford University Press.
- Watts, D. J. and Strogatz, S. H. (1998). Collective dynamics of ‘small-world’ networks. *nature*, 393(6684):440–442.
- Xia, M., Wang, J., and He, Y. (2013). Brainnet viewer: a network visualization tool for human brain connectomics. *PLoS one*, 8(7):e68910.
- Yu, K., Wang, X., Li, Q., Zhang, X., Li, X., and Li, S. (2018). Individual morphological brain network construction based on multivariate euclidean distances between brain regions. *Frontiers in human neuroscience*, 12:204.
- Zhang, J., Feng, F., Han, T., Duan, F., Sun, Z., Cai, C. F., and Solé-Casals, J. (2021). A hybrid method to select morphometric features using tensor completion and f-score rank for gifted children identification. *Science China Technological Sciences*, 64(9):1863–1871.